Exact study of charge-spin separation, pairing fluctuations, and pseudogaps in four-site Hubbard clusters

Armen N. Kocharian*
Department of Physics and Astronomy, California State University, Northridge, California 91330-8268, USA

Gayanath W. Fernando†
Department of Physics, University of Connecticut, Storrs, Connecticut 06269, USA
and IFS, Hantana Road, Kandy, Sri Lanka

Kalum Palandage
Department of Physics, University of Connecticut, Storrs, Connecticut 06269, USA

James W. Davenport
Computational Science Center, Brookhaven National Laboratory, Upton, New York 11973, USA
(Received 15 October 2005; revised manuscript received 12 April 2006; published 17 July 2006)

An exact study of charge-spin separation, pairing fluctuations, and pseudogaps is carried out by combining the *analytical* eigenvalues of the four-site Hubbard clusters with the grand canonical and canonical ensemble approaches in a multidimensional parameter space of temperature (T), magnetic field (h), on-site interaction (U), and chemical potential (μ). Our results, near the average number of electrons $\langle N\rangle \approx 3$, strongly suggest the existence of a critical parameter $U_c(T)$ for the localization of electrons and a particle-hole binding (*positive*) gap $\Delta^{e\text{-}h}(T)>0$ at $U>U_c(T)$, with a zero temperature critical value, $U_c(0)=4.584$. For $U<U_c(T)$, the particle-particle pair binding is found with a (*positive*) pairing gap $\Delta^{P}(T)>0$. The ground state degeneracy is lifted at $U>U_c(T)$ and the cluster becomes a Mott-Hubbard like insulator due to the presence of energy gaps at all (allowed) integer numbers ($1\leq N\leq 8$) of electrons. In contrast, for $U\leq U_c(T)$, we find an electron pair binding instability at finite temperature near $\langle N\rangle \approx 3$, which manifests a possible pairing mechanism, a precursor to superconductivity in small clusters. Rigorous criteria for the existence of many-body Mott-Hubbard like particle-hole and particle-particle pairings, spin pairing, (spin) pseudogap, and (spin) antiferromagnetic critical crossover temperatures, at which the corresponding pseudogaps disappear, are also formulated. In particular, the resulting phase diagram consisting of charge and spin pseudogaps, antiferromagnetic correlations, hole pairing with competing hole-rich ($\langle N\rangle=2$), hole-poor ($\langle N\rangle=4$), and magnetic ($\langle N\rangle=3$) regions in the ensemble of clusters near 1/8 filling closely resembles the phase diagrams and inhomogeneous phase separation recently found in the family of doped high-T_c cuprates.

DOI: 10.1103/PhysRevB.74.024511 PACS number(s): 65.80.+n, 73.22.−f, 71.27.+a, 71.30.+h

I. INTRODUCTION

Understanding the effects of electron correlation and pseudogap phenomena[1–6] in doped oxides, including the cuprate superconductors, is one of the most challenging problems in condensed matter physics.[7] Although the experimental determination of various inhomogeneous phases in cuprates is still somewhat controversial,[8] the underdoped high-T_c superconductors (HTSCs) are often characterized by crossover temperatures below which excitation pseudogaps in the normal state are seen to develop.[9] In these materials, the spectral weight begins to be strongly suppressed below some characteristic temperature T_s that is higher than the superconducting crossover temperature T_c. There are many experiments supporting a highly nonuniform hole distribution leading to the formation of hole-rich and hole-poor regions in doped $La_{2-x}Sr_xCuO_4$ and other cuprate HTSCs.[10] This electronic phase separation is expected to be mostly pronounced at low hole concentrations. Recently, strong experimental evidence has been found for "electronic phase separation" in La cuprates near optimal doping into separate, magnetic, and superconducting phases.[11]

The relevance of the Hubbard model for studies of the HTSCs has been the focus of intensive research and debated for quite some time with no firm conclusions up to now. Even though the small Hubbard clusters do not have the full capacity to describe the complexity of copper ions and their ancillary oxygens detected in the HTSC materials, it is still argued that this model can capture the essential physics of the HTSCs.[1] However, except in one and infinite dimensions, there is no exact solution currently available for the Hubbard Hamiltonian. It is also known that in the optimally doped cuprates, the correlation length of dynamical spin fluctuations is very small,[12] which points to the local character of electron interactions in the cuprates. Therefore, exact microscopic studies of pairing, crossover, and pseudogaps, by using analytical diagonalization of small Hubbard clusters, which account accurately for short-range dynamical correlations, are relevant and useful with regard to understanding the physics of the HTSCs. Our exact analytical solution appears to be providing useful insight into the physical origin of the high-energy insulator metal and low-energy antiferromagnetic crossovers, electron pairing, and spin density fluctuations in the superconducting phase.

The following questions are central to our study: (i) When treated exactly, what essential features can the simple Hubbard clusters capture that are in common with the HTSCs? (ii) Using simple cluster studies, is it possible to obtain a mesoscopic understanding of electron-hole and/or electron-electron pairing and identify various possible phases and crossover temperatures? (iii) Do these small clusters (coupled to a particle bath) contain important features that are similar to large clusters and thermodynamical systems?

Our work has uncovered important answers to the questions raised above. This is a follow-up to our recent study, in which rigorous criteria were found for the existence of Mott-Hubbard (MH) and Neél type bifurcations, corresponding critical temperatures of crossovers and various phases in finite-size systems.[13] Small two- and four-site clusters with short-range electronic correlations provide (unique) insight into the thermodynamics and exact many body physics, difficult to obtain from approximate methods. In particular, we show that these small Hubbard clusters, in the absence of long-range order, exhibit particle-particle, Mott-Hubbard like particle-hole and/or antiferromagnetic-paramagnetic instabilities at finite temperature.

In addition, the four-site (square) cluster is the basic building block of the CuO_2 planes in the HTSCs and it can be used as a block reference to build up larger superblocks in two dimensions of desirable sizes by applying cluster perturbation theory (CPT),[14] nonperturbative real-space renormalization group (RSRG),[15] contractor renormalization group (CORE),[16] or dynamical cluster approximation (DCA) for embedded four-site clusters coupled to an uncorrelated bath.[17] Similar attempts at studying small clusters (such as the ground state studies of weakly coupled Hubbard dimers and squares by Tsai and Kivelson[18]) have begun recently and the lessons learned here will be invaluable to such studies and useful to the condensed matter community in general. Above all, these small clusters can be synthesized and utilized for understanding essential many-body physics at the mesoscopic level and hence are useful in their own right.

II. MODEL AND METHODOLOGY

The single orbital four-site minimal Hubbard Hamiltonian,

$$H = -t\sum_{i\sigma}(c^{+}_{i\sigma}c_{i+1\sigma} + \mathrm{H.c.}) + U\sum_{i} n_{i\uparrow}n_{i\downarrow} - h\sum_{i} S^{z}_{i}, \quad (1)$$

with hopping t and on-site interaction U is the focus of this work. Periodic boundary conditions are used for the clusters. Unless otherwise stated, all the energies reported here are measured in units of t (i.e., t has been set to 1 in most of the equations that follow). Our calculations are based on the exact *analytical* expressions for the eigenvalue E_n of the nth many-body eigenstate of the four-site Hubbard clusters.[19] As we show here, this model used in conjunction with the grand canonical and canonical ensembles yields valuable insights into the physics of strongly correlated electrons.

A. Thermodynamics and response functions

The complete phase diagram of interacting electrons can be obtained with high accuracy due to the analytically (exact) given thermodynamic expressions. In Fig. 1, possible electron configurations (below half filling) in the grand canonical ensemble for the four-site clusters are shown. The grand partition function Z_U (where the number of particles N and the projection of spin s^z are allowed to fluctuate) and its derivatives are calculated (exactly) without taking the thermodynamic limit. The exact grand canonical potential Ω_U for many-body interacting electrons is

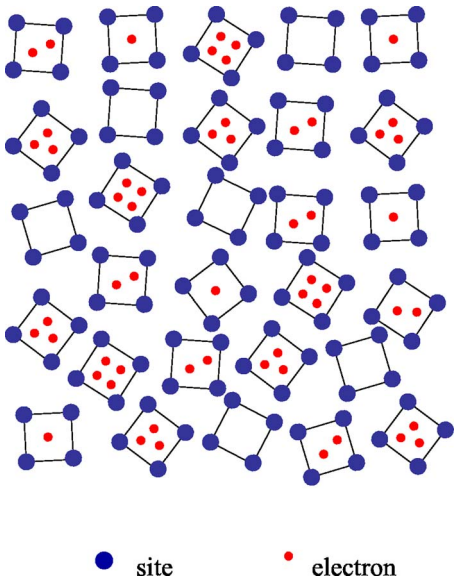

FIG. 1. (Color online) Various possible configuration mixing of electrons (below half filling) that can be found in an ensemble of four-site clusters. Note that the mixing of configurations is brought about by the temperature.

$$\Omega_U = -T\ln\sum_{n\le N_H} e^{-(E_n-\mu N_n - hs^z_n)/T}, \quad (2)$$

where N_n and s^z_n are the number of particles and the projection of spin in the nth state respectively. The Hilbert space dimension in Eq. (2) is $N_H=4^4$. The derivatives we study may be labeled as first order (such as the average spin projection and/or magnetization in response to an applied magnetic field) or second order (such as fluctuations and/or susceptibilities). These responses, evaluated as functions of chemical potential μ, applied field h, on-site Coulomb interaction U, and temperature T, carry a wealth of information that can be used to identify various phases and phase boundaries. Some of these results for the two- and four-site clusters were reported earlier in Ref. 13.

The (first order) responses due to doping and external magnetic field are as follows:

$$\langle N\rangle = -\frac{\partial\Omega_U}{\partial\mu}, \quad (3)$$

$$\langle s\rangle = -\frac{\partial\Omega_U}{\partial h}. \quad (4)$$

Analytical expressions derived for the averages $\langle N\rangle$ and $\langle s\rangle$ are analyzed numerically in a wide range of U, h, μ, and T

parameters. The charge and spin degrees respond to an applied magnetic field (h) as well as electron or hole doping levels (i.e., chemical potential μ) and display clearly identifiable, prominent peaks, paving the way for rigorous definitions of MH, antiferromagnetic (AF), spin pseudogaps, and related crossover behavior.[13] The exact expressions for charge susceptibility $\chi_c = \frac{\partial \langle N \rangle}{\partial \mu}$ and spin susceptibility $\chi_s = \frac{\partial \langle s^z \rangle}{\partial h}$ can be found from

$$\langle X^2 \rangle - \langle X \rangle^2 = T \frac{\partial \langle X \rangle}{\partial x}, \tag{5}$$

where X corresponds to N or s^z and x to μ or h. Using maxima and minima in spin and charge susceptibilities, phase diagrams in a T versus μ plane for any U and h can be constructed. This approach also allows us to obtain quantum critical points and rigorous criteria for various transitions, such as the MH like transition, using the evolution of peaks in charge or spin susceptibility[13] (see below).

B. Charge (pseudo)gap

We define canonical energies $\mu_\pm$,

$$\mu_+ = E(M+1, M'; U{:}T) - E(M, M'; U, T), \tag{6}$$

$$\mu_- = E(M, M'; U{:}T) - E(M-1, M'; U{:}T), \tag{7}$$

where $E(M, M'; U{:}T)$ is the canonical (ensemble) energy with a given number of electrons $N = M + M'$ determined by the number of up (M) and down (M') spins. At zero temperature the expressions (6) and (7) are identical to those introduced in Ref. 20. At finite temperature, the calculated charge susceptibility is a differentiable function of N and μ. The peaks (i.e., maxima) in $\chi_c(\mu)$, *which may exist in a limited range of temperature*, are identified easily from the conditions $\chi_c'(\mu_\pm) = 0$ with $\chi_c''(\mu_\pm) < 0$. We define $T_c(\mu)$ to be the temperature at which a (possible) peak is found in $\chi_c(\mu)$ at a given μ.

The positive charge gap for electron-hole (exciton) excitations, $\Delta^{e\text{-}h}(T) > 0$, is defined by

$$\Delta^{e\text{-}h}(T) = \begin{cases} \mu_+ - \mu_- & \text{if } \mu_+ > \mu_- \\ 0 & \text{otherwise} \end{cases} \tag{8}$$

as the separation between μ_+ and μ_-. The electron-hole instability $\Delta^{e\text{-}h}(T) \geq 0$ can exist in a limited range of temperatures and $U \geq U_c(T)$, with $\Delta^{e\text{-}h}(T) \equiv 0$ at $U \leq U_c(T)$. [In general, the critical parameter $U_c(T)$, identified and discussed in Secs. III A and III B, depends also on h.] The energy gap, $\Delta^{e\text{-}h}(T) \geq 0$, serves as a natural order parameter in a multidimensional parameter space h, U, T and at $T \neq 0$ will be called a *pseudogap*, since χ has a small, but nonzero weight inside the gap. At $T = 0$, this gap $\Delta_0^{e\text{-}h} \equiv \Delta^{e\text{-}h}(0)$ will be labeled a *true gap* since $\chi_c$is exactly zero inside.

The difference $\mu_+ - \mu_-$ is somewhat similar to the difference $I - A$ for a cluster, where I is the ionization potential and A the electron affinity. For a single isolated atom at half filling and $T = 0$, $I - A$ is equal to U and hence the above difference represents a screened U, reminiscent of Herring's definition of U in transition elements.[21]

C. Mott-Hubbard crossover

The thermodynamic quantities with fixed N (*canonical approach*) are certainly smooth, analytical functions of T and U. Thus one may naively think that at half filling there is no real cooperative phenomena at $T \sim U$ for transition from localized to delocalized electrons or at $T \sim \frac{t^2}{U}$ for transition from antiferromagnetic to paramagnetic state. At finite temperature, the thermodynamic quantities Ω_U and $\langle N \rangle$ are both analytic and smooth functions of T and μ. Although the charge susceptibility χ_c is also a differentiable function of μ and T at all $T > 0$, χ_c versus μ exhibits a weak transition at some critical temperature T_{MH} (*saddle point*).[13] Thus the MH crossover at half filling can be defined simply as a critical temperature T_{MH}, at which two peaks merge into one with $\mu = \mu_+ = \mu_- = U/2 = \mu_0$ and $\chi_c'(\mu) = 0$ and $\chi_c''(\mu) = 0$, i.e., as the temperature corresponding to a point of inflexion in $\chi_c(\mu)$.[13] This procedure gives a rigorous definition for the MH crossover temperature T_{MH} (from a localized into an itinerant state), at which the electron-hole pseudogap melts, i.e., $\Delta^{e\text{-}h}(T_{\mathrm{MH}}) = 0$. The MH crossover, due to its many-body nature, is also a cooperative effect which may occur even for a single atom.

D. Spin (pseudo)gap

Analogously, we define a (positive) spin pairing gap between various spin configurations (projections of spin s^z) for a given number of electrons in the absence of a magnetic field as

$$\Delta^s(T) = E(M+1, M'-1; U{:}T) - E(M, M'; U{:}T). \tag{9}$$

This corresponds to the energy necessary to make an excitation by overturning a single spin. Possible peaks in the zero magnetic field spin susceptibility $\chi_s(\mu)$, when monitored as a function of μ, can also be used to define an associated temperature, $T_s(\mu)$, as the temperature at which such a peak exists and the spin pseudogap as the separation between two such peaks.

E. AF (pseudo)gap and onset of magnetization

Similar to the (charge) plateaus seen in $\langle N \rangle$ versus μ, we can trace the variation of magnetization $\langle s^z \rangle$ versus an applied magnetic field h and identify the spin plateau features, which can be associated with staggered magnetization or short-range antiferromagnetism. We calculate the critical magnetic field $h_{c\pm}$ for the onset of magnetization ($s^z \to \pm 0$), which depends on N and μ, by flipping a down spin, $h_{c+} = E(M+1, M'-1; U{:}T) - E(M, M'; U{:}T)$ or an up spin, $h_{c-} = E(M, M'; U{:}T) - E(M-1, M'+1; U{:}T)$.[22] The spin singlet binding energy $\Delta^{\mathrm{AF}}(T) > 0$ can be defined as

$$\Delta^{\mathrm{AF}}(T) = \frac{h_{c+} - h_{c-}}{2}, \tag{10}$$

and serves as a natural antiferromagnetic order parameter in a multidimensional parameter space U, T, μ. This will be called an AF pseudogap at nonzero temperature. We define T_{AF} as the temperature at which the pseudogap, $\Delta^{\mathrm{AF}}(T) = 0$,

vanishes and above which a paramagnetic state is found. An exact analytical expression for the AF spin gap in the ground state $[\Delta^{\mathrm{AF}}(0)]$ at half filling was obtained in Ref. 13. In what follows, all of the temperatures defined above, $T_c(\mu)$, $T_s(\mu)$, and $T_{\mathrm{AF}}(\mu)$, will be used when constructing phase diagrams.

F. Pairing instability

To determine whether the cluster can support electron pairing at finite temperature despite the purely repulsive electronic interactions, the electron-electron (or hole-hole) pair binding energy

$$\Delta^P(T) =$$

$$[E(M-1,M';U{:}T) - E(M+1,M';U{:}T)] -$$

$$2[E(M,M';U{:}T) - E(M+1,M';U{:}T)] \qquad (11)$$

is calculated by adding or subtracting one electron near $N=M+M'$. The average energy $E(M,M';U{:}T)$ is given for configurations with a fixed number of electrons N and spin magnetization $s=0$ using our grand canonical ensemble approach. At zero temperature, the binding energy (11) is identical to the one introduced in Ref. 23.

Using the definitions for $\mu_{\pm}$ from Eqs. (6) and (7), electron-electron (or hole-hole) pair energy can also be written as

$$\Delta^P(T) = \begin{cases} \mu_- - \mu_+ & \text{if } \mu_- > \mu_+ \\ 0 & \text{otherwise.} \end{cases} \qquad (12)$$

In the ground state, the electron-pair binding energy gap is fully developed when $\Delta^P(0)>0$, i.e., $\mu_->\mu_+$, which leads to an effective attraction between the electrons for $U \le U_c(T)$.[24] *On the other hand, when* $\mu_+>\mu_-$, *the condition* $\Delta^{e\text{-}h}(T)>0$ *with* $U>U_c(T)$ *provides an electron-hole pairing mechanism as a precursor to antiferromagnetism.*[13] We can define T_P as the temperature at which the pseudogap $\Delta^P(T_P)=0$ vanishes. The existence of particle-particle $[\Delta^P(T)>0]$ or particle-hole $[\Delta^{e\text{-}h}(T)>0]$ instability and the corresponding solution for a positive pseudogap $[\Delta(T)>0]$ can be formulated by combining both Eqs. (8) and (12) in one for any $U>0$ as

$$\Delta(T) = \begin{cases} \Delta^{e\text{-}h}(T) & \text{if } U > U_c(T) \\ \Delta^P(T) & \text{if } U < U_c(T). \end{cases} \qquad (13)$$

At zero temperature, $\Delta(0)=0$ at $U=0$ or $U=U_c(0)$.

III. RESULTS

A. $\langle N\rangle$ and $\langle s^z\rangle$ versus μ and pseudogaps

In Fig. 2, we explicitly illustrate the variation of $\langle N\rangle \le 4$ versus μ for various U values in order to track the variation of charge gaps with U. The opening of such gaps is a local correlation effect and clearly does not follow from long-range order, as exemplified here. The true gaps at $\langle N\rangle=1$ and $\langle N\rangle=4$ develop for infinitesimal $U>0$ and increase monotonically. In contrast, the charge gap at $\langle N\rangle=3$ opens at finite

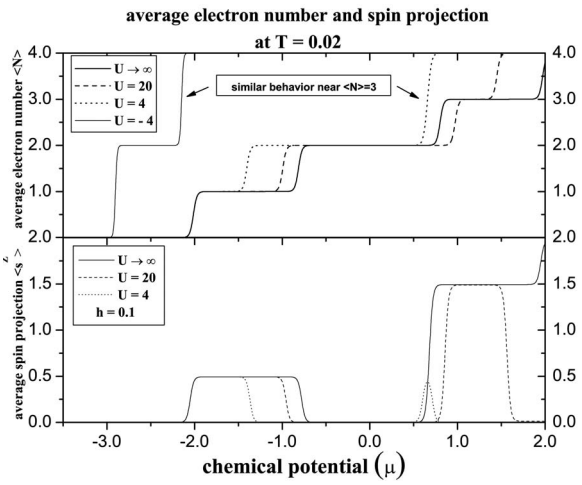

FIG. 2. Variation of average electron concentration $\langle N\rangle$ (above) and average spin $\langle s^z\rangle$ (below) vs μ for various U values at temperature $T=0.02$. The vanishing of the charge gap near $\langle N\rangle=3$ for $U=4$ has implications related to pairing as discussed in the text. Note also that the spin plot has been obtained with an applied magnetic field of $h=0.1$ and shows the stabilization of a magnetic state near $\langle N\rangle=3$ for $U=4$. At zero field, $\langle s^z\rangle=0$ everywhere due to degeneracy between spin up and down states.

$U>U_c(T)$ (see Fig. 2). Thus at low temperature, $\langle N\rangle$ (expressed as a function of μ in Fig. 2) evolves smoothly for $U \le U_c(T)$, showing finite leaps across the MH plateaus only at $\langle N\rangle=1$, $\langle N\rangle=2$. Such a density profile of $\langle N\rangle$versus μ near $\langle N\rangle=3$ closely resembles the one calculated in Fig. 2 for the *attractive* four-site Hubbard cluster with $U=-4$ at $T=0.02$ and is indicative of a possible particle pairing instability. At larger $U>U_c(T)$, an electron-hole gap is opened at $\langle N\rangle=3$. Therefore the cluster at $U>U_c(0)$ behaves as a MH like insulator at all (allowed) integer numbers $(1 \le N \le 8)$ with electron charge localized (non-Fermi liquid). In contrast, at $U \le U_c(0)$ the chemical potential gets pinned upon doping in the midgap states at $\langle N\rangle \simeq 3$.

While Fig. 2 shows the magnetization at a relatively high magnetic field, its behavior at very low temperature, $T \to 0$, and infinitesimal magnetic field, $h \to 0$, is also noteworthy. In this case, as U increases, $\langle N\rangle$ and $\langle s^z\rangle$ versus μ near $\langle N\rangle=3$ reveal islands of stability for various charge (N) and spin (s,s^z) configurations as follows. Phase A $[U \le U_c(0)]$: particle-particle $\Delta^P(0)>0$ and spin $\Delta^{s^z=0}(0)>0$ pairing gaps with the minimal spin projection $\langle s^z\rangle=0$ (*singlet pairing*) state. Phase B $[U_c(0)<U<4(2+\sqrt{7}) \simeq 18.583]$: particle-hole $\Delta^{e\text{-}h}(0)>0$ and spin-spin $\Delta^{s^z=1/2}(0)>0$ pairings with unsaturated spin $\langle s^z\rangle=1/2$ (*triplet pairing*). Phase C [large $U>4(2+\sqrt{7})$]: particle-hole $\Delta^{e\text{-}h}(0)>0$ pairing without spin gap $[\Delta^{s^z=3/2}(0) \equiv 0]$ and maximum spin $\langle s^z\rangle=3/2$ (saturated ferromagnetism, Ref. 25).

In phase A for $U=4$, charge and spin are coupled (i.e., no charge-spin separation), while in phase B at $U=6$, the charge and spin are partially decoupled (partial charge-spin separation). In phase C for $U \to \infty$, the charge and spin are fully decoupled, when the charge gap saturates to its maximum

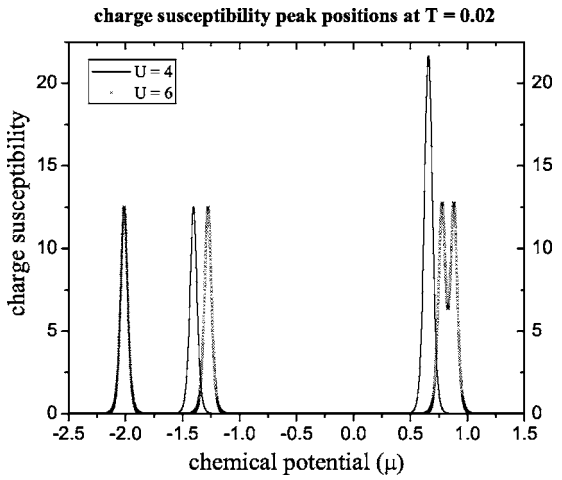

FIG. 3. The charge susceptibility vs chemical potential μ at $T=0.02$ for two different U values ($U=4$ and $U=6$) below half filling. Note that there are clearly identifiable peaks, and such peak positions, when monitored as a function of temperature, have been used to construct phase diagrams (see text).

value, $\rightarrow 2(2-\sqrt{2})$, while the spin gap from $\langle s^z\rangle = 1/2$ to $\langle s^z\rangle = 3/2$, defined earlier in Eq. (9), vanishes (full charge-spin separation coupling with double electron). Phase A is due to strong particle-particle coupling with double electron charge ($Q=2e$) and zero spin ($s^z=0$) excitation coupling here and is a good candidate for the full "bosonization" of charge and spin degrees of freedom and possible "superconductivity." In contrast, at even numbers of electrons, $\langle N\rangle \simeq 2$, in Fig. 2 there are electron-hole $\Delta^{e\text{-}h}(0)\neq 0$ and spin $\Delta^{s^z=0}(0)\neq 0$ pairings at all U values, and therefore the charge and spin are coupled and there is full charge-spin reconciliation, when the *singlet-triplet* spin excitation gap at quarter filling approaches the charge gap, $\Delta^{s^z=0}\equiv\Delta^{e\text{-}h}=2(2\sqrt{2}-1)$, as $U\rightarrow\infty$. Exactly at half filling, $\langle N\rangle=4$, there is a charge-spin separation at all finite $U>U_c$. However, as $U\rightarrow\infty$, the charge gap $\Delta^{e\text{-}h}(0)\rightarrow\infty$ and $\Delta^{s^z=0}(0)\rightarrow 0$ vanishes, there is no charge-spin separation in this limiting case. Also, we find that for all U at $\langle N\rangle=1$, the charge gap $\Delta^{e\text{-}h}(0)\neq 0$, while spin gap $\Delta^{s=1/2}(0)\equiv 0$. For any given N one can also easily identify an insulator or a "metallic" liquid if $\Delta^{e\text{-}h}(0)\neq 0$ or a $\Delta^{e\text{-}h}(0)\equiv 0$ in the charge sector. It is also useful to distinguish the spin insulator, $\Delta^{s^z=0}(0)\neq 0$, or spin liquid,$\Delta^{e\text{-}h}(0)\equiv 0$, state in the spin sector accordingly.

In Fig. 3, we show the evolution of charge susceptibility χ_c as a function of μ, which exhibits clearly identifiable sharp peaks. At low temperature, peak structures in $\chi_c(\mu)$ and zero magnetic field spin susceptibility $\chi_s(\mu)$ are observed to develop in these clusters; between two consecutive peaks, there exists a pseudogap in charge or spin degrees. The opening of such distinct and separated pseudogap regions for spin and charge degrees of freedom (at low temperature) is a signature of corresponding charge and spin separation away from half filling.

B. Pairing gap at $\langle N\rangle=3$

At relatively large $U\geq U_c(T)$, the energy gap $\Delta_3^c(U:T)=E(4;U:T)+E(2;U:T)-2E(3;U:T)$ becomes positive for

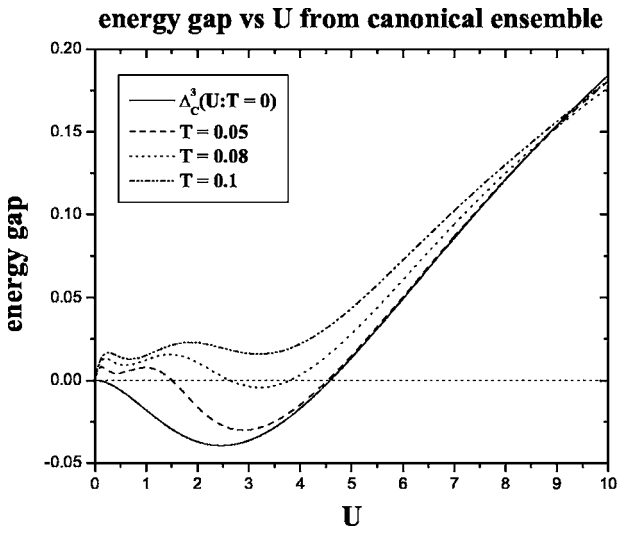

FIG. 4. The energy gap given by Eq. (14) at zero temperature and its evolution at several nonzero temperatures as a function of U obtained from the canonical ensemble. This is directly related to the electron-electron pairing gap $[U<U_c(T)]$ and electron-hole charge gap $[U>U_c(T)]$ as defined in the text. Note that charge pairing is unlikely to occur above temperature $T=0.08$. As previously mentioned, all energies are measured in units of t, the hopping parameter.

$\langle N\rangle=3$ (see Fig. 4). Its zero temperature value and analytical expression were first derived in Ref. 13 as

$$\Delta_3^c(U:T=0) = -\frac{2}{\sqrt{3}}\sqrt{(16t^2+U^2)}\cos\frac{\gamma}{3}+\frac{U}{3} - \frac{2}{3}\sqrt{(48t^2+U^2)}\cos\frac{\alpha}{3} + \sqrt{32t^2+U^2+4\sqrt{64t^4+3t^2U^2}}, \tag{14}$$

where $\alpha=\arccos\left\{\left(\frac{4Ut^2}{3}-\frac{U^3}{27}\right)/\left(\frac{16t^2}{3}+\frac{U^2}{9}\right)^{3/2}\right\}$ and $\gamma=\arccos\left\{(4Ut^2)/\left(\frac{16t^2}{3}+\frac{U^2}{3}\right)^{3/2}\right\}$. Due to (ground state) level crossings,[25] the exact expression (14) is valid only in a limited range of $U\leq 4(2+\sqrt{7})$. The critical value, $U_c(0)=4.583\,999\,38$, at which $\Delta_3^c(U_c:T=0)=0$, first reported in Ref. 13, serves as an estimation of the accuracy of the gap value.

When $\Delta_3^c(U:T)=E(4;U:T)+E(2;U:T)-2E(3;U:T)$ becomes negative for $U\leq U_c(T)$ as shown in Fig. 4, the $\langle N\rangle=3$ states become less (energetically) favorable when compared with $\langle N\rangle=2$ and $\langle N\rangle=4$ states. This is a manifestation of electron binding where, despite bare electron repulsion, electron pairs experience an attraction.[18,23,24] We have also observed a similar vanishing of charge gaps for negative U values (see Fig. 2), where there is an inherent electron-electron attraction, supporting the above statement. For $U\geq U_c(T)$, the gap in the electron-hole channel is positive [i.e., $\Delta_3^c(T)>0$] which favors excitonic, electron-hole pairing, similar to MH gap at half filling.

C. Phase separation

It appears that the canonical approach yields an adequate estimation of a possible pair binding instability in the ensemble of small clusters at relatively low temperature. The competition between attraction and repulsion under hole doping can lead to a "microscopic phase separation," which is comprised of an inhomogeneous structure of competing and coexisting hole rich $\langle N\rangle=2$ (hole-hole or electron-electron pairing), hole poor $\langle N\rangle=4$ (AF at half filling), and magnetic $\langle N\rangle=3$ clusters. It is apparent that the condition $\mu_-=\mu_+$ at $U=U_c(0)$ and $\langle N\rangle=3$ from Eqs. (6) and (7) defines a lower bound for the existence of phase separation boundary, that distinguishes a charge-spin separated region from a charge-spin coupled one.

If we neglect every second hopping term in the two-dimensional square lattice, the system can be thought of as an ensemble of decoupled four-site noninteracting clusters,[16,18] as shown in Fig. 1. Important features appear if the number of electrons $\langle N\rangle=3$ and total magnetization $\langle s^z\rangle=0$ are kept fixed for the whole system of decoupled clusters, placed in the (particle) bath, by allowing the particle number on each separate cluster to fluctuate. One is tempted to think that due to symmetry, there is only a single hole on each cluster within the $\langle N\rangle=3$ ensemble. However, this statement reflects a simple average only. Due to thermal and quantum fluctuations in the density of holes between the clusters [for $U<U_c(T)$], it is energetically more favorable to form pairs of holes. In this case, snapshots of the system at relatively low temperatures and at a critical value (μ_P in Fig. 5) of the chemical potential would reveal equal probabilities of finding (only) clusters that are either hole-rich $\langle N\rangle=2$ or hole-poor $\langle N\rangle=4$.

However, at higher temperatures when pairing coexists with magnetic spin fluctuations, there exists a small window of parameters which brings some stability to $\langle N\rangle=3$ clusters. The crossover from full separation (segregation) to the coexisting magnetic ($\langle N\rangle=3$) and hole-rich ($\langle N\rangle=2$) phases develops smoothly and depends on the degree of disorder, i.e., temperature. In Sec. III A, it was shown how the changes in the parameter U affect the spin (magnetization) by changing the cluster configuration.

Phase separation of magnetic $\langle N\rangle=3$ and paired states $\langle N\rangle=2$ can also be triggered by increasing the magnetic field. The phase separation (i.e., *segregation*) into separate magnetic $\langle N\rangle=3$ and hole-rich $\langle N\rangle=2$ regions, seen here at μ_- $>\mu_+$, closely resembles the phase separation effect detected recently in superoxygenated $La_{2-x}Sr_xCuO_{4+y}$, with various Sr contents.[11] Thus our results are consistent with the experimental observation that a small (applied) magnetic field mimics doping and promotes stability of the magnetic phase $\langle N\rangle=3$ over the superconducting state $\langle N\rangle=2$ near optimal doping.

In addition, our calculated probabilities (from the grand canonical ensemble) at low temperature show that, in the interval $\mu_+<\mu<\mu_P$, $\langle N\rangle=2$ clusters become the majority; i.e., we observe both pairing and phase separation at low temperature. Note that phase separation here has a different origin and occurs at relatively weak coupling $U<U_c$ far from the level crossing regime, at which the spin gap vanishes. Therefore, the mechanism of phase separation here is different from the one found in Refs. 26 and 27 at large U limit due to the *spin* density fluctuations ($h_+<h_-$) and *spin* saturation. Indeed, the four-site cluster at large $U>4(2+\sqrt{7})$ reveals ferromagnetism in accordance with the Nagaoka theorem.[25]

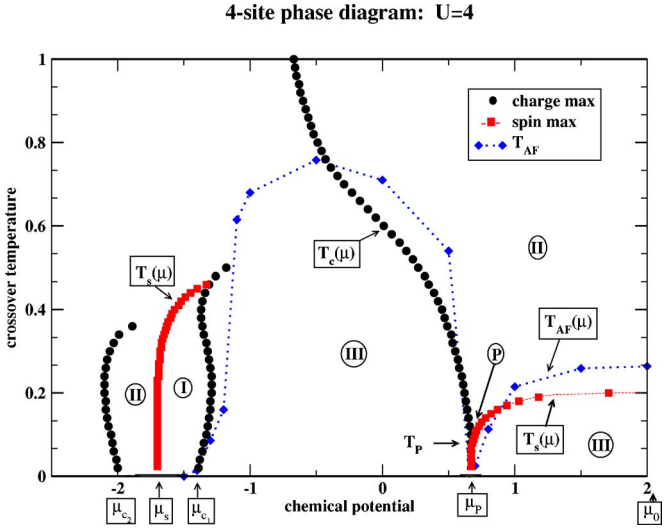

FIG. 5. (Color online) Temperature T vs chemical potential μ phase diagram for the four-site cluster at $U=4$ and $h=0$, below half filling ($\mu\leq\mu_0$). Regions I and II are paramagnetic phases and quite similar to the ones found in the two-site cluster (Ref. 13), showing strong charge-spin separation. Phase III is a MH antiferromagnetic phase (with zero spin). However, note the (new) line phase (labeled P) which consists of charge and spin fluctuations. This is a new feature seen in the four-site cluster which suggests the existence of electron-electron pairing and phase separation into hole-rich and hole-poor regions at low temperature. For $U=4$, pairing occurs below the temperature, $T_P=0.076$.

D. Phase diagrams

In Figs. 5 and 6, phase diagrams for the four-site cluster ($U=4$ and $U=6$) are shown (see also Ref. 28). These have been constructed almost exclusively using the temperatures, $T_c(\mu)$, $T_s(\mu)$, and $T_{\rm AF}(\mu)$, defined previously. We have identified the following phases in these diagrams: (I) and (II) are MH like paramagnetic phases with a charge pseudogap separated by a phase boundary where the spin susceptibility reaches a maximum, with $\Delta^{e\text{-}h}(T)>0$, $\Delta^{\rm AF}\equiv 0$; at finite temperature, phase I has a higher $\langle N\rangle$ compared to phase II; phase (III) is a MH like antiferromagnetic insulator with bound charge and spin, when $\Delta^{e\text{-}h}(T)>0$, $\Delta^{s}(T)>0$, $\Delta^{\rm AF}(T)>0$; (P) is a line phase for $U=4$ with a vanished charge gap at $\langle N\rangle=3$, now corresponding to the opening of a pairing gap $[(\Delta^{P}(T)>0)]$ in the electron-electron channel with $\Delta_3^c(U:T)<0$. We have also verified the well-known fact that the low-temperature behavior in the vicinity of half filling, with charge and spin pseudogap phases coexisting, represents an AF insulator.[13] However, *away from half filling*,

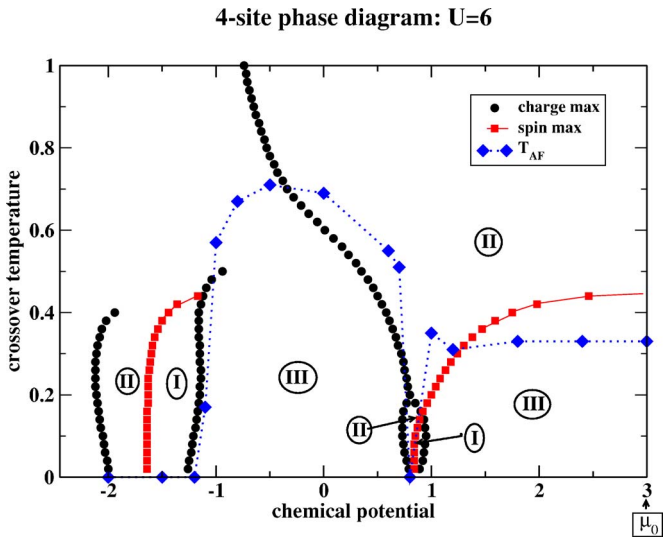

FIG. 6. (Color online) Temperature T vs the chemical potential μ phase diagram for the four-site cluster at $U=6$ and $h=0$, below half filling ($\mu \leq \mu_0$). Regions I, II, and III are quite similar to the ones found for $U=4$ in Fig. 5, again showing strong charge-spin separation. However, a charge gap opens as a new bifurcation (I and II phases) which consists of charge and spin pseudogaps (replacing the equilibrium line phase P in the previous figure, i.e., no electron-electron pairing here: see text for details). Temperature labels similar to those shown in Fig. 5 may be used here but have been suppressed for clarity.

we find very intriguing behavior in thermodynamical charge and spin degrees of freedom.

In both phase diagrams, we find similar paramagnetic MH (I), (II) charge-spin separated phases in addition to the AF (III) phase where spin and charge are bounded. In Fig. 6, spin-charge separation in phases (I) and (II) originates for relatively large $U(=6)$ in the underdoped regime. In contrast, Fig. 5 shows the existence (at $U=4$) of a line phase (with pairing) similar to $U<0$ case with electron pairing $[\Delta^P(T) > 0]$, when the chemical potential is pinned up on doping within the highly degenerate midgap states near (underdoped) 1/8 filling.

E. Quantum critical points

Among other interesting results, rich in variety, sharp transitions at quantum critical points (QCP) near $\langle N \rangle = 3$ are found in the ground state at $U > U_c(0)$ between phases with true charge and spin gaps; for infinitesimal $T \to 0$, these gaps are transformed into pseudogaps with some nonzero weight between peaks (or maxima) in susceptibilities monitored as a function of doping (i.e., μ) as well as h. In the limiting case $T_c(\mu_c) \to 0$, the QCP doping, μ_c, defines a sharp MH like (AF) transition with diverging χ_c.[13] At the QCP doping μ_s, with $T_s(\mu_s) \to 0$, the zero spin susceptibility, χ_s also exhibits a maximum.

In Fig. 6, the critical temperature $T_s(\mu)$ falls abruptly to zero at the QCP doping μ_s [true only for $U > U_c(0)$], implying[8] that the (spin) pseudogap can exist independently of possible particle pairing in Fig. 6. In contrast, for $U < U_c(0)$ and low temperature, there is no charge-spin separation near $\langle N \rangle = 3$. Therefore in Fig. 5 at $U=4$ $[U < U_c(0)]$ we do not observe any QCP associated with μ_s or μ_c close to $\langle N \rangle = 3$. Instead, Fig. 5 shows the existence of a line phase (with pairing) similar to the attractive $U<0$ case with a spin pseudogap, which exists only at finite temperature $T_s(\mu) > 0$, and electron pairing $(T_P > T_s)$,when the chemical potential is pinned up on doping within the highly degenerate midgap states near (underdoped) 1/8 filling.

We have also seen that a reasonably strong magnetic field can bring about phase separation and has a dramatic effect (mainly) on the QCP at μ_s, at which the spin pseudogap disappears. It is evident from our exact results that the presence of QCP at zero temperature and critical crossovers at $T_c(\mu)$, $T_s(\mu)$, and $T_{\mathrm{AF}}(\mu)$ temperatures, gives strong support for the cooperative character of existing phase transitions and crossovers similar to those seen in large thermodynamic systems at finite temperatures.[29,30]

F. Charge-spin separation

The charge-spin separation effect is fundamental for understanding of the generic features common for small and large thermodynamic systems. We formulated exact criteria when the charge and spin excitations are decoupled at $U > U_c(T)$. There is controversy regarding the nature of MH and AF transitions and relation between their consequent critical temperatures.[13] In Figs. 5 and 6 MH charge decoupled from spin degree of freedom condenses at temperatures below T_c, while AF spin correlations are seen to develop at lower temperatures $T_{\mathrm{AF}}(\mu) < T_c(\mu)$ (Ref. 13). Until recently electrons were thought to carry their charge and spin degrees of freedom equally; however, accurate studies of thermodynamic response functions in nanoscale clusters show that in real materials, these two degrees of freedom are relatively independent from one another and can condensate at different doping levels μ_c, μ_s and transition temperatures $T_c(\mu)$, $T_{AF}(\mu)$, and $T_s(\mu)$ shown in Fig. 5 and 6.

The charge-spin separation is an unusual behavior of electrons in some materials under certain conditions permitting the formation of two independent (bound) electron-electron or electron-hole pairs (quasiparticles) in charge sectors and spin singlet and triplet states in spin sectors. The spin quasiparticle only carries the spin degree of the electron but not the charge, while the charge quasiparicle has spin equal to zero but its electric charge equals either zero (electron-hole pair) or a charge of two electrons (electron-electron pair). We find that at large $U > U_c(T)$, clusters with localized charge are favored over itinerant ones.

As an important footnote, in the noninteracting $U=0$ case shown in Fig. 7, the charge and spin peaks follow one another (in sharp contrast to the $U=4$ and 6 cases). In regions I and II, positions of charge (as well as spin) maxima and minima coincide indicating that there is no charge-spin separation, even in the presence of a magnetic field. In the entire range of μ, the charge and spin fluctuations directly follow one another without charge-spin separation. Our detailed analysis of the (responses such as) variation of electron concentration $\langle N \rangle$, zero magnetic field magnetization $\langle s^z \rangle$ versus

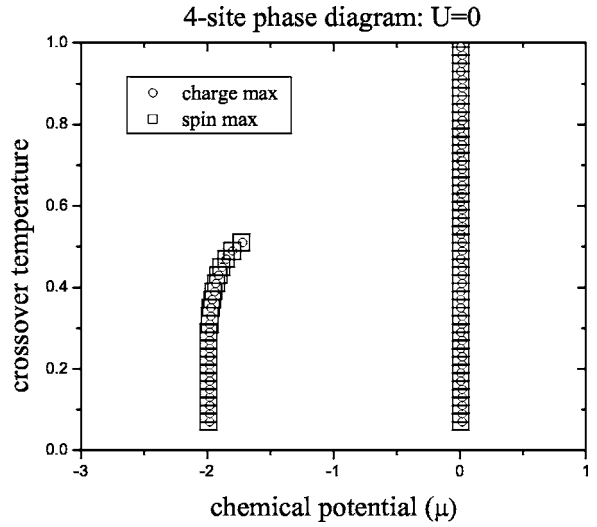

FIG. 7. The single particle or "noninteracting" ($U=0$) case, illustrating the positions of charge and spin susceptibility peaks in a $T-\mu$ space for the four-site cluster for $\mu<1$ (half filling is at $\mu_s=0$). Note how the charge and spin peaks follow one another. Even in the presence of a nonzero magnetic field there is no charge-spin separation.

μ and various fluctuations shows that there is no charge-spin separation and both the spin and charge degrees closely follow each other. Thus, at $U=0$ the spin and charge degrees are strongly coupled to one another. On the other hand, the charge-spin separation effect at $U\neq 0$ led to rigorous definitions of Mott-Hubbard like, antiferromagnetic, spin pseudogaps, particle-particle pairing, and related crossovers.

IV. CONCLUSION

In summary, we have illustrated how to obtain phase diagrams and identify the presence of temperature driven crossovers, quantum phase transitions, and charge-spin separation for any $U\geq 0$ in the four-site Hubbard *nanocluster* as doping (or chemical potential) is varied. Specifically, our exact solution pointed out an important difference between the $U=4$ $[U<U_c(0)]$ and $U=6$ $[U>U_c(0)]$ phase diagrams at finite temperature in the vicinity of hole doping $\approx 1/8$ which can be tied to possible electron-electron pairing due to overscreening of the repulsive interaction between electrons in the former. The resulting phase diagram for $U<U_c(0)$ with competing hole-rich ($\langle N\rangle=2$), hole-poor ($\langle N\rangle=4$), and magnetic ($\langle N\rangle=3$) phases captures also the essential features of phase separation in doped $La_{2-x}Sr_xCuO_{4+y}$.[11] Our analytical results near $\langle N\rangle\approx 3$ suggest strongly that particle pairing can exist at $U<U_c(T)$, while particle-hole binding is presumed to occur for $U>U_c(T)$. It is also clear that short-range correlations alone are sufficient for pseudogaps to form in small and large clusters, which can be linked to the generic features of phase diagrams in temperature and doping effects seen in the HTSCs. The exact cluster solution shows how charge and spin (pseudo) gaps are formed at the microscopic level and their behavior as a function of doping (i.e., chemical potential), magnetic field, and temperature. The pseudogap formation can also be associated with the condensation of spin and charge degrees of freedom below spin and charge crossover temperatures. In addition, our exact analytical and numerical calculations provide important benchmarks for comparison with Monte Carlo, RSRG, DCA, and other approximations.

Finally, our results on the existence of QCP and crossover temperatures show the *cooperative nature* of phase transition phenomena in finite-size clusters similar to large thermodynamic systems. The small *nanoclusters* exhibit a pairing mechanism in a limited range of U, μ, and T and share very important intrinsic characteristics with the HTSCs apparently because in all these "bad" metallic high-T_c materials, local interactions play a key role. As charge and spin fluctuations are relevant to the charge and spin susceptibilities (5), energy fluctuations are related to the specific heats and these new results for the four-site and larger clusters, which provide further support to our picture developed here, will be reported elsewhere.

ACKNOWLEDGMENTS

One of us (A.N.K.) wishes to thank Steven Kivelson for his interest and communicating the results of Ref. 18 prior to publication. This research was supported in part by the U.S. Department of Energy under Contract No. DE-AC02-98CH10886.

*Electronic address: armen.n.kocharian@csun.edu
†Electronic address: fernando@phys.uconn.edu

[1] P. W. Anderson, Science **235**, 1196 (1987).
[2] V. Emery and S. A. Kivelson, Nature (London) **374**, 434 (1995).
[3] T. Timusk and B. Statt, Rep. Prog. Phys. **62**, 61 (1999).
[4] S. A. Kivelson, I. P. Bindloss, E. Fradkin, V. Oganesyan, J. M. Tranquada, A. Kapitulnik, and C. Howald, Rev. Mod. Phys. **75**, 1201 (2003).
[5] D. S. Marshall, S. A. Kivelson, I. P. Bindloss, E. Fradkin, V. Oganesyan, J. M. Tranquada, A. Kapitulnik, and C. Howald, Phys. Rev. Lett. **76**, 4841 (1996).
[6] Andrea Damascelli, Zahid Hussain, and Zhi-Xun Shen, Rev. Mod. Phys. **75**, 473 (2003).
[7] P. W. Anderson, Adv. Phys. **46**, 3 (1997).
[8] G. V. M. Williams, J. L. Tallon, and J. W. Loram, Phys. Rev. B **58**, 15053 (1998).
[9] V. J. Emery, S. A. Kivelson, and O. Zachar, Phys. Rev. B **56**, 6120 (1997).
[10] M. Matsuda, M. Fujita, K. Yamada, R. J. Birgeneau, Y. Endoh, and G. Shirane, Phys. Rev. B **65**, 134515 (2002).
[11] H. E. Mohottala, B. O. Wells, J. I. Budnick, W. A. Hines, C. Niedermayer, L. Udby, C. Bernard, A. R. Moodenbaugh, and Fang-Cheng Chou, Nature (London) **5**, 377 (2006).
[12] Y. Zha, V. Barzykin, and D. Pines, Phys. Rev. B **54**, 7561 (1996).

[13] A. N. Kocharian, G. W. Fernando, K. Palandage, and J. W. Davenport, J. Magn. Magn. Mater. **300**, 585 (2006).
[14] D. Sénéchal, D. Perez, and M. Pioro-Ladriere, Phys. Rev. Lett. **84**, 522 (2000).
[15] Jean-Paul Malrieu and Nathalie Guihery, Phys. Rev. B **63**, 085110 (2001).
[16] E. Altman and A. Auerbach, Phys. Rev. B **65**, 104508 (2002).
[17] M. Jarrell, Th. Maier, M. H. Hettler, and A. N. Tahvildarzadeh, Europhys. Lett. **56**, 563 (2001).
[18] Wei-Feng Tsai and Steven A. Kivelson, Phys. Rev. B **73**, 214510 (2006); Bull. Am. Phys. Soc. (March 2006-u44.00006).
[19] R. Schumann, Ann. Phys. **11**, 49 (2002).
[20] E. H. Lieb and F. Y. Wu, Phys. Rev. Lett. **20**, 1445 (1968).
[21] C. Herring, in *Magnetism* edited by G. T. Rado and H. Suhl (Academic Press, New York, 1966), Vol. IV.
[22] A. N. Kocharian and Joel H. Sebold, Phys. Rev. B **53**, 12804 (1996).
[23] R. M. Fye, M. J. Martins, and R. T. Scalettar, Phys. Rev. B **42**, R6809 (1990); J. E. Hirsch, S. Tang, E. Loh, Jr., and D. J. Scalapino, Phys. Rev. Lett. **60**, 1668 (1988).
[24] Steven R. White, Sudip Chakravarty, Martin P. Gelfand, and Steven A. Kivelson, Phys. Rev. B **45**, 5062 (1992).
[25] D. C. Mattis, Int. J. Nanosci. **2**, 165 (2003).
[26] P. B. Visscher, Phys. Rev. B **10**, 943 (1974).
[27] V. J. Emery, S. A. Kivelson, and H. Q. Lin, Phys. Rev. Lett. **64**, 475 (1990).
[28] A. N. Kocharian, G. W. Fernando, K. Palandage, and J. W. Davenport, cond-mat/0510609 (unpublished).
[29] W. Langer, M. Plischke, and D. M. Mattis, Phys. Rev. Lett. **23**, 1448 (1969).
[30] M. Cyrot, Phys. Rev. Lett. **25**, 871 (1970).